UNIVERSIDAD EAFIT

Vigilada Mineducación

THERMODYNAMIC ANALYSIS OF CO_2 REMOVAL PROCESS BY ADSORPTION ON NaX

Análisis termodinámico del proceso de remoción de CO_2 mediante adsorción en NaX

SEBASTIÁN SERQUERA MESA
LAURA ORTEGA ARCILA

Proyecto de grado

Asesor, docente
Santiago Builes Toro

UNIVERSIDAD EAFIT
ESCUELA DE INGENIERÍAS
INGENIERÍA DE PROCESOS
MEDELLÍN
2021

Thermodynamic analysis of CO_2 removal process by adsorption on NaX

Sebastian Serquera Mesa[a] , Laura Ortega Arcila[a]

Santiago Builes Toro[b]

[a] *Processs Engineering Student, EAFIT University, Medellín, Colombia*
[b]*Professor, Project Advisor, Department of Process Engineering, EAFIT University, Medellín, Colombia*

Abstract

The continuous increase of carbon dioxide concentration in the atmosphere is the main contributor to climate change. Thus, it is imperative to develop strategies that help to control manmade emissions of this gas. Carbon dioxide capture is an intensive research area that aims to decrease the energy requirements for the separation and storage of CO_2. Even though absorption using an aqueous solvent is a well-established and is the most widely implemented capture technology, it requires high energy for the regeneration of the solvent due to the need to increase the temperature of the aqueous solvent, decreasing the overall efficiency of the process. Adsorption using porous solids has been presented as an alternative process to capture CO_2 while decreasing the energy requirements.

In the present work, a thermodynamic analysis of the CO_2 removal process by adsorption using literature reported data is performed, in order to devise a framework to evaluate and compare two adsorbents under realistic process conditions. Zeolites NaX and Beta were used as case studies to evaluate the proposed model. The results show that, although bed composition profiles have similar trends for both adsorbents, there is a significant difference in the regeneration temperature of these adsorbents, since for zeolite NaX the regeneration temperature is reached around 360K when CO_2 is almost pure, whereas for Beta this value is reached around 390K. Thus, NaX has a lower energy requirement than Beta for stablished process conditions. The energy penalty is 91.08 MW per molCO_2 recovered for NaX and 104.28 MW per molCO_2 recovered for Beta, which is consistent with the calculation of the specific thermal energy and the working capacity.

1. Introduction

According to the International Energy Agency [1], global CO_2 emissions reached a historical high of 33.5 Gt in 2018, of which power generation together with transport, accounted for over two thirds. These emissions contribute around 75% to the global greenhouse gas emissions in CO_2e [2]. This has caused environmental problems such as increase of ~1 degree Celsius in the earth's average surface temperature since 1900 [3, 4], an average loss of 407 billion tons of ice per year in Greenland and Antarctica between 1993 and 2016 [5], and a global sea level rise of ~20 cm in the last century [6].

The close link between power generation and CO_2 emissions means that while energy demand continues to increase, CO_2 emissions will also increase. In 2017, global electricity demand grew by 3%, more than any other energy source, reaching 22.2 petawatt-hours [7] because of economic growth. Although new technologies for energy production have been developed, renewable energies represent only 26% of the global energy production [8]. For instance, wind and solar photovoltaic now provide around 6% of the electricity generation worldwide [7]. However, this is still inadequate to supply the increasing global energy demand and it is expected that the

non-renewable energies remain as the major component of the energy mix at least in the mid-term [7]. Hence, it is necessary to implement a mid-term solution to mitigate climate change due to anthropogenic CO_2 emissions.

Therefore, research to develop processes that increase the efficiency of capture systems are critical to create a feasible greenhouse gas emission control plan, covering not only power plants and industrial facilities but also the infrastructure required to support that plan [9].

The development of carbon capture, utilization, and storage technologies (CCUS) could constitute part of that solution [10-13] particularly if current research in this area is able to achieve significant cost reductions. For instance, 18 large-scale CCUS projects are in operation globally today, capturing around 33 million tons of CO_2 each year (~0.1% of the global emissions).

The most common capture technology is absorption with aqueous solutions of amines [14, 15]. Despite that, an important barrier to the deployment of any aqueous amine solvents is the high energy required for solvent regeneration [16-18]. On the other hand, adsorption can avoid the need to heat liquids with large heat capacities by directly heating the gas phase potentially lowering the energy requirement [13]. This process is a surface-dominated capture mechanism taking place when CO_2 meets a solid adsorbent through physical interactions. Adsorption is commonly implemented for post-combustion processes, that is after the fuel has been burned. Here, the flue gas is recovered from the emission source, containing 3-15 mol % CO_2 [19], depending on the fuel. The recovered gas then goes through a cyclic adsorption process in which adsorption and desorption steps are performed to separate and store the CO_2 and regenerate the adsorbent. The capture units are expected to concentrate the CO_2 from flue gas with purity and recovery exceeding 95 and 90% respectively [20, 21], the purity gives an idea of the desired product concentration in the flue gas, which is CO_2 for this case; and the recovery refers to the amount of original substance that is recovered after a chemical process is completed.

In addition to purity and recovery there are other relevant metrics to evaluate CCUS projects. For instance, the specific thermal energy requirement, which is the amount of heat required during the heating step per unit production of the desired product; or the cyclic working capacity, which is the molar amount of the desired product recovered per cycle per unit mass of adsorbent. Another very important parameter, which can be derived from the aforementioned metrics, is the energy penalty, which is the relationship between the energy required to capture CO_2 and the energy produced in the plant when generating the CO_2.

As mentioned above, even if in principle the regeneration energy required can be lower in adsorption than in absorption, this requires the use of adsorbents with high selectivity and high capacity. Thus, currently there are not commercial examples of well-structured adsorption processes for CO_2 capture from low pressure flue gas streams [23, 24]. Most research on adsorbents for CO_2 capture have focused on exploring the adsorption and separation capabilities of different materials. Even today it is still a materials science challenge to find/synthesize an adsorbent that covers all the critical specifications with respect to CO_2 for their implementation in an industrial process [25]. Although there are a large number of works in the literature describing the characteristics of adsorbents for CO_2 capture [26-29], there is no a common framework for the evaluation of those materials from the process' point of view.

A step in the development of an evaluation of adsorbents at a process level was that of Ajenifuja et al. [30]. They developed a simplified temperature swing adsorption (TSA) model for a three-step cycle. The algorithm allowed rapid screening of adsorbents for the recovery of strongly adsorbed species from a gas mixture. Purity, recovery, specific thermal energy demand, and cyclic working capacity were the indicators used to evaluate zeolite NaX and 75 other adsorbents performance for post-combustion CO_2 capture. Even though there is a large number of published CO_2 adsorption data with different types of adsorbents [31-35], there is not an established step-by-step mechanism to evaluate these adsorption isotherms from different sources considering their application in industrial removal of CO_2.

The need to reduce the energy penalty of CCUS technologies required for decarbonization of energy generation process and the need to have a simple and reliable evaluation tool to assess the energy requirements of a given adsorbent are the main drivers for this project. The aim of this work is analyzing thermodynamically the CO_2 removal by adsorption using data from adsorption isotherms. Herein, zeolites NaX and Beta are used as case studies to evaluate the method using previously published data. First, a framework to evaluate and

compare adsorbents for CO_2 capture under realistic TSA process conditions is proposed. Then, the developed method is used to determine the penalty energy required for a sample carbon capture process taking information from experimental data of zeolites NaX and Beta.

2. Materials and methods

The current work considers the flue gases to be treated in the adsorption process as a binary mixture containing CO_2 (a strongly adsorbing component) and N_2 (a weakly adsorbing component). This assumption can be explained because the gaseous products from coal combustion are mostly CO_2 (14.98%), N_2 (76.54%), O_2 (2.32%), H_2O (6.13%), and SO_2 (0.002%) [36], where CO_2 represents the interest compound, and the N_2 corresponds to the mostly abundant compound. However, the model could be extended to consider multicomponent mixtures by making appropriate modifications to the mass and energy balance equations.

This work considers a TSA cycle, two-bed, three-step with indirect heating and cooling system [30], as shown in Figure 1. This process typically operates at atmospheric pressure (or near), but the model can operate under any isobaric conditions. The TSA process consists of three steps (i) adsorption, (ii) heating, and (iii) cooling.

- Adsorption: the cycle starts with an empty adsorption bed. The flue gases are fed from one end of the column. The CO_2 is preferentially adsorbed by the zeolites, significantly decreasing the CO_2 concentration in the outlet at the other end of the adsorption column. This behavior continues until the adsorbent saturates and an increase in the CO_2 concentration in the outlet is observed.
- Heating: once the adsorbent saturates the flue gas inlet is closed, the temperature is increased, and the outlet remains open for the recovery of the CO_2.
- Cooling: after the CO_2 has been desorbed at the desired temperature the temperature is decreased while closing the outlet and opening the inlet of the adsorption column, this stage ends once the adsorption temperature is reached, and the cycle is repeated until a cyclic steady state is obtained.

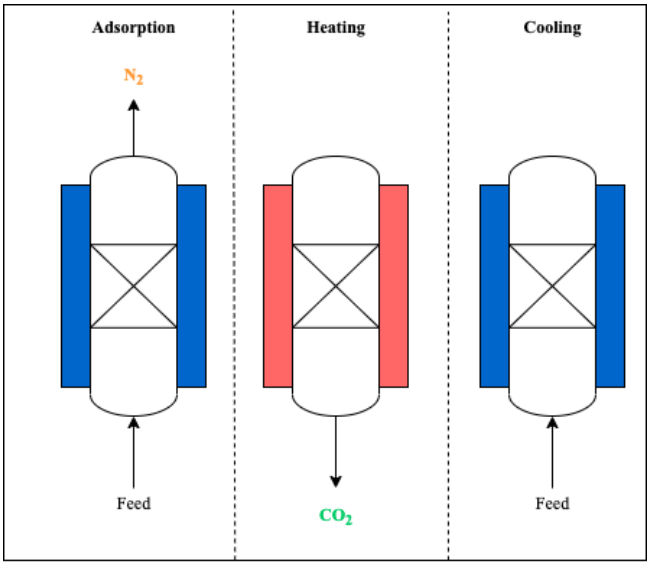

Figure 1. Schematic of the three-step TSA cycle process. Blue means a heating fluid flows through the jacket while red means a cooling fluid flows

The adsorption equilibrium dictates the saturation capacity during the adsorption step and the temperature swing required for the heating and cooling step. This information is obtained from adsorption isotherm, which is an equilibrium expression relating the concentration of the fluid phase to the concentration of the adsorbed particles at a given temperature [37].

In order to calculate the energy requirement of the carbon capture process, a mathematical model was developed. This model was divided in two sections. In the first one, a shortcut model was adopted to describe the mass and heat transfer in each step of the TSA cycle and evaluate the adsorbents' performance. In the second one, the adsorption isotherm experimental data from literature were used to fit the parameters that describe the equilibrium behavior of a binary system in the two adsorbents. Finally, a study-case process was adopted to evaluate both adsorbents under realistic process conditions.

2.1. Adsorption process modeling

The mass and heat transfer in each step of the TSA cycle were modeled to evaluate the adsorbents' performance using the shortcut model proposed by Ajenifuja et al. [30]. The simplifying assumptions proposed in that work significantly reduce the computational complexity compared to a full detailed model and its accuracy to predict process performance across the range of operating conditions investigated. The simplifying assumptions are as follows:

- The bed is well-mixed during the heating and cooling steps; that is, there are no axial or radial temperature or concentration gradients within the bed.
- During the adsorption step, a discontinuous profile separating the initial concentration from the feed concentration propagates through the bed until breakthrough.
- The pressure drop in the bed is negligible.
- The adsorbed and gas phases are in thermal and chemical equilibrium.
- Heat-transfer resistances are negligible.
- The specific heat capacity of the gas phase is negligible.
- The gas phase is accurately described by the ideal gas law.

The assumption of instantaneous heat transfer and of a discontinuous front during the adsorption step means that at the end of the adsorption step, the gas-phase composition in the bed is identical to the feed composition, and the bed is at the adsorption temperature. The model is summarized below.

The overall material balance around an adsorption column containing X components is given by

$$\sum_{i=1}^{X} N_{j,total}^{0} + N_{in} - N_{out} = \sum_{i=1}^{X} N_{j,total}^{f} \tag{1}$$

Where $N_{j,total}$ is the sum of the total moles of the component *i* in the adsorbed phase and the total moles of the component *i* in the gas phase. The superscripts "0" and "f" refer to the initial and final states of the column, N_{in} is the total moles fed into the bed, and N_{out} is the total moles removed from the bed.

The energy balance is given by

$$m_1 H_1 = m_2 H_2 + Q_{ext} \tag{2}$$

Where m_1 and m_2 are the total mass of the adsorbent in states 1 and 2 respectively, H_1 and H_2 are the enthalpies of the adsorbent in states 1 and 2 respectively and Q_{ext} is the amount of external heating or cooling provided.

Considering that in adsorption process, the energy changes (ΔH) that occur in the bed are quantified by the isosteric heat of adsorption, and that for states 1 and 2 the total mass of the adsorbent are equal ($m_1 = m_2 = m$), eq 2 could be expressed as:

$$m c_{p,ads} \Delta \mathrm{T} = \sum_{i=1}^{X} \Delta H_{is,i}\, \Delta N_{i,ads} + Q_{ext} \tag{3}$$

Where $c_{p,\,ads}$ is the specific heat capacity of the adsorbent, ΔT is the change in the column temperature, $\Delta H_{is,i}$ is the isosteric heat of adsorption of the component *i*, $\Delta N_{ads,i}$ is the change in moles adsorbed of the component *i*.

The dependence of the isosteric heat of adsorption on temperature and adsorbed phase loading is represented by a Clapeyron-type expression

$$\Delta H_{is,i} = \mathrm{R}T^2 \left(\frac{d(\ln P_i)}{dT} \right)_{q_i} \tag{4}$$

Where *T* is the adsorption temperature, P_i is the partial pressure of the component *i* and q_i is the amount adsorbed of component *i* from the gas mixture. Eq 4 was solve numerically in Excel with a pressure delta of 1Pa while temperature delta was 0.1K.

Adsorbent performance was analyzed by the specific thermal energy requirement and the cyclic working capacity. These parameters allow a comparation in thermodynamic terms of the performance of a given adsorbent in the adsorption process. However, other performance indicators, such as product purity and recovery, were evaluated too.

The shortcut TSA model was implemented using Python version 3.8.8. The heating and cooling steps were divided into 50 sub-steps. For heating and cooling steps and for the overall adsorption step, the applicable system of equations described in Figure 2 were solved for each sub-step *k*. Subscripts A and B refers to CO_2 and N_2 respectively; T_{ads} is the adsorption temperature; T_{des} is the desorption temperature; y_A is the gas-phase mole fraction of component "A"; ε is the total porosity; m is the mass of the adsorbent; ΔT^k is the temperature change between current and previous sub-steps; $\Delta N_{i,ads}^k$ is the change in moles adsorbed of the component *i* between current and previous sub-steps; superscripts *cool* and *BT* refers to the end of the cooling and adsorption steps respectively; and N_{waste} is the total moles of the undesired product, which is rich in the weakly adsorbed component and recovered during the adsorption step.

The solver requires initial guesses for the solution of the system of equations. The heating step was computed first, with initial CO_2 composition equal to the feed composition. At each sub-step, the calculated values from the previous sub-step were used in the solver as initial guesses for the solution of the system of equations.

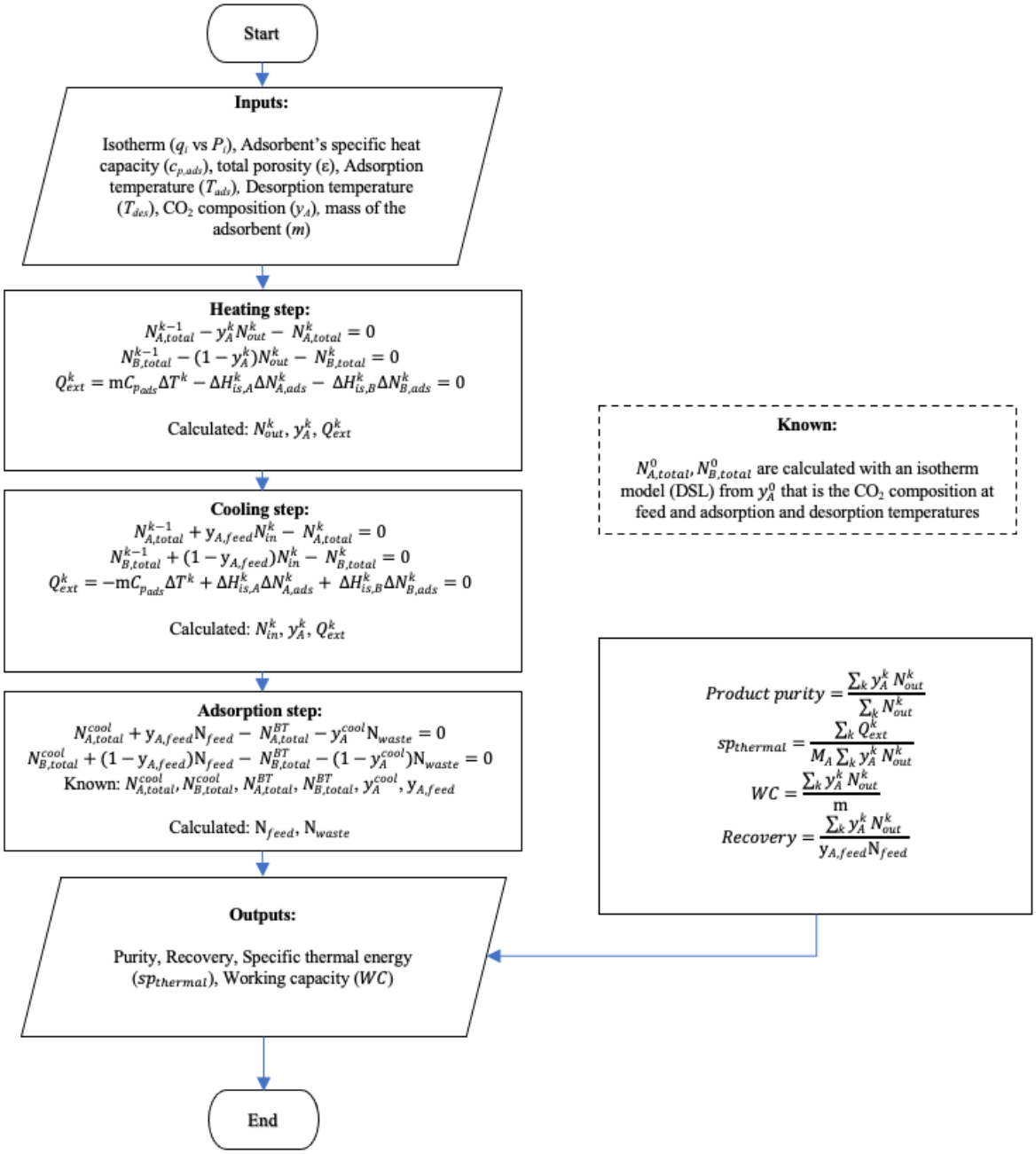

Figure 2. Flowchart of the algorithm used to solve the shortcut model of CO_2 capture process.

2.2. Dual-site Langmuir isotherm model

The dual-site Langmuir (DSL) model was selected to fit the parameters that describe the equilibrium behavior. This adsorption model allows the prediction of the equilibrium behavior of binary and ternary systems reasonably well using parameters obtained from fits to the pure component equilibrium data [30].

This model describes the adsorption of a pure component on a heterogeneous adsorbent that is composed of two homogeneous but energetically different sites [38-40]. The adsorbed amount, q, of the component *i*, would be given by

$$q_i = \frac{q_{s1,i} b_i P_i}{1 + b_i P_i} + \frac{q_{s2,i} d_i P_i}{1 + d_i P_i} \tag{5}$$

Were $q_{sn,i}$ is the saturation capacity of *i* at the adsorption site *n*; P_i is the partial pressure of *i*; b_i and d_i are the affinity parameters of *i* for sites 1 and 2, respectively, which are considered to be temperature dependent as expressed in equations 6 and 7, where $b_{0,i}$ and $d_{0,i}$ are the pre-exponential factors; $Q_{1,i}$ and $Q_{2,i}$ are their corresponding adsorption energies; R is the universal gas constant; and T is the adsorption temperature.

$$b_i = b_{0,i} \exp\left(\frac{Q_{1,i}}{RT}\right) \tag{6}$$

$$d_i = d_{0,i} \exp\left(\frac{Q_{2,i}}{RT}\right) \tag{7}$$

It is necessary to relate the interactions between all the components in the gas mixture. The DSL model has different cases for a multicomponent system. It is important to consider the energetic site-matching issue to correctly apply the DSL formulation. The energetic site-matching issue refers to the fact that in a multicomponent system all the adsorbates do not necessarily see the site 1 as the high-free-energy site and site 2 as the low-free energy site. For a binary system, two possible forms of the extended DSL exist: perfect positive (PP), where both adsorbates see the same site as the high energy site, and perfect negative (PN), where the adsorbates see different sites as the high energy site [41]. As CO_2 and N_2 have similar sizes, unless otherwise stated, the PP form of the binary DSL isotherm model was used in this work, and it is described in eq 8.

$$q_i = \frac{q_{s1,i} b_i P_i}{1 + \sum_{j=1}^{n} b_j P_j} + \frac{q_{s2,i} d_i P_i}{1 + \sum_{j=1}^{n} d_j P_j} \tag{8}$$

Where subscript *j* refers to the components in the gas mixture from 1 to *n.* Fitting of the model to the experimental data was done with Excel, and the values of the parameters for each component were found by minimizing the sum of the mean relative errors (MRE).

2.3. Case-study process conditions

In this work we adapted a sample process reported for a pulverized coal (PC)-fired power plant [36], which is commonly used in power generation plants. In that process, CO_2 capture and compression are the final unit operations in a CCUS process with aqueous amines. For simplicity, we are not going to consider the compression of CO_2 but focus the analysis on the CO_2 capture step adapting it to a CO_2 adsorption process with zeolites NaX and Beta. Table 1 shows the parameters reported for the PC-fired power plant that are considered in this work as the reference case study conditions to demonstrate the application of the proposed algorithm.

Table 1. Reference parameters for the evaluation of the separation process using the zeolites NaX and Beta [36]

Technical parameters	Value
Net output (MW)	800.00
Coal consumption (kg/s)	61.00
Auxiliary work (MW)	42.13
Net efficiency (%)	40.38
CO_2 emission (kg/s)	164.41
Flue gas flow (kg/s)	725.00
CO_2 concentration of flue gas (%mol)	14.98
Capture efficiency (%)	90.00

3. Results and analysis

3.1. Model development

3.1.1. Fitted adsorption isotherm model

The experimental data for the fitting was taken from two different sources. As it is shown below in Figure 3, points correspond to experimental data, filled symbols [42] and open symbols [28]. The initial guesses for the fitting procedure were the parameters reported by Ajenifuja et al. [30]. That fact can explain the closeness of MRE sum values to cero. For instance, the maximum MRE sum was 0.051 for NaX and 0.063 for Beta. However, it is important to note that the experimental data have an uncertainty, and it could affect the fitting results. It is important to use reliable and robust methods for fitting the experimental data, and for datasets without initial values it is recommended to at least use the values for a similar reported material.

The goodness of fit to the experimental data can also be seen in Figure 3 where the experimental absolute adsorption isotherms of pure CO_2, N_2 on zeolites NaX and Beta, shown as symbols, are very close to the simulated data, shown as lines.

As expected, CO_2 always adsorbs more strongly than N_2 on both adsorbents for all temperatures. It is shown in Figure 3, where the adsorbed amount of CO_2 is higher for all pressure changes. The affinity parameters, *b* and *d*, are larger for CO_2 than the corresponding ones for N_2 for both adsorbents at all temperatures, which means that CO_2 is more strongly attracted to the adsorbent active sites than N_2. Adsorption is an exothermic process, therefore the affinity parameters decrease with temperature, so at higher temperature the isotherms become less sharply curved. That is why all adsorbent performance indicators have a strongly dependence of adsorption and desorption temperatures, and process conditions are critical factors when choosing a certain adsorbent for a given application.

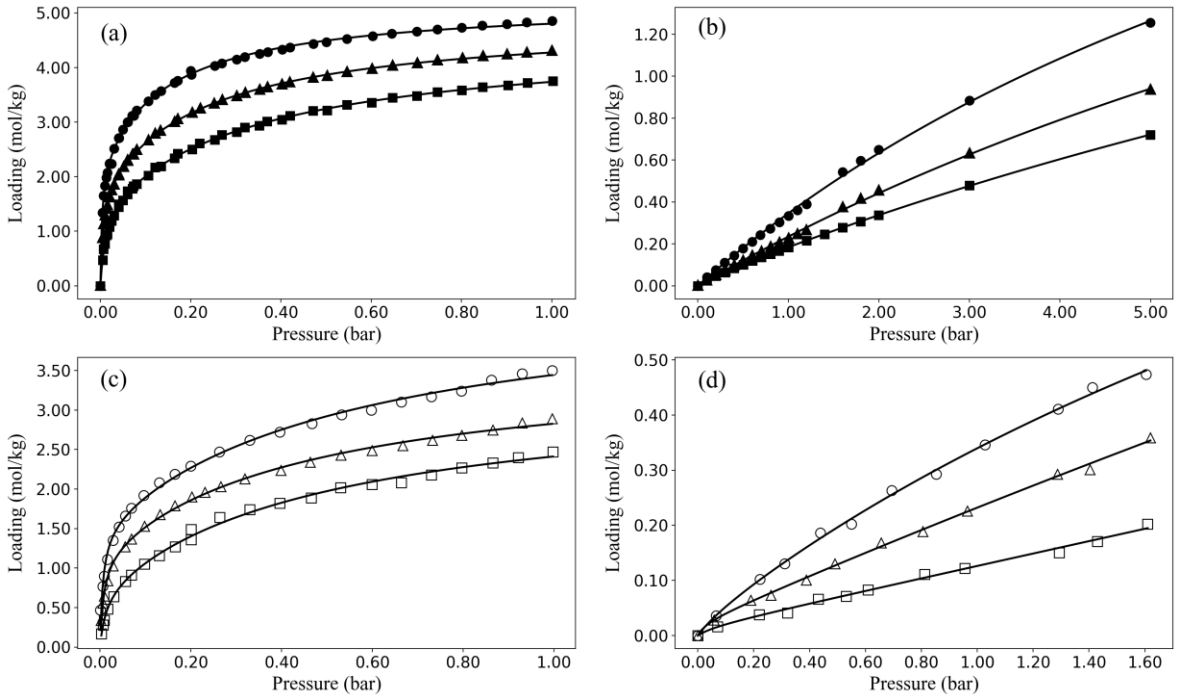

Figure 3. Fitting of pure CO_2 and N_2 adsorption data at different temperatures (Symbols: experimental data: circles 298K; triangles 313K; squares 333K. Lines: fitted DSL model): (a) CO_2 in NaX, (b) N_2 in NaX, (c) CO_2 in Beta, (d) N_2 in Beta.

From a thermodynamic consistency point of view, the saturation capacity ($q_{sn,i}$) for each component should not be temperature-dependent [41]. Hence, this restriction must be included in the adsorption model. Three adsorption datasets at different temperatures were used to fit the parameters of DSL model for each component at the two adsorbents, and they are presented in Table 2 and Table **3**.

Table 2. DSL model parameters for single-component adsorption on zeolite NaX

Component	$q_{s1,i}$ (mol/kg)	$q_{s2,i}$ (mol/kg)	$b_{0,i}$ (bar^{-1})	$d_{0,i}$ (bar^{-1})	**293 K**		**313 K**		**333 K**	
					b_i (bar^{-1})	d_i (bar^{-1})	b_i (bar^{-1})	d_i (bar^{-1})	b_i (bar^{-1})	d_i (bar^{-1})
CO_2	2.50	3.18	2.23×10^{-8}	1.13×10^{-7}	23.79	1.33	8.83	0,51	3.69	0.22
N_2	3.16	3.16	9.57×10^{-6}	9.57×10^{-6}	1.91	1.91	1.06	1.06	0.63	0.63

Table 3. DSL model parameters for single-component adsorption on zeolite Beta.

Component	$q_{s1,i}$ (mol/kg)	$q_{s2,i}$ (mol/kg)	$b_{0,i}$ (bar^{-1})	$d_{0,i}$ (bar^{-1})	**293 K**		**313 K**		**333 K**	
					b_i (bar^{-1})	d_i (bar^{-1})	b_i (bar^{-1})	d_i (bar^{-1})	b_i (bar^{-1})	d_i (bar^{-1})
CO_2	6.32	29.08	1.01×10^{-6}	8.83×10^{-6}	1.64	2.87	0.66	1.16	0.06	0.04
N_2	2.50	2.50	8.89×10^{-6}	8.89×10^{-6}	0.11	0.11	0.07	0.07	0.03	0.03

3.1.2. Shortcut model development

The DSL model was used to calculate the total loading of each component in all steps of the TSA shortcut model at stablished process conditions. The cyclic behavior of the three stages adsorption process is presented in Figure 4 for both zeolites NaX and Beta. The adsorption column cycles through these three steps until it reaches a cyclic steady state. At cyclic steady state, the profiles of the bed internal temperature, composition, and pressure no longer change between cycles, and a consistent product is recovered in subsequent cycles [43]. For both adsorbents, composition profiles have similar trends. For instance, the isotherm process is seen in the adsorption step, where CO_2 composition increases at the same temperature until breakthrough, while in the heating step the CO_2 composition starts to increase with temperature until reaches the desorption temperature where the CO_2 tends to a value close to one. Even though the bed composition profiles have similar trends for both adsorbents, there is a significant difference in the regeneration temperature of both adsorbents. For NaX, the regeneration temperature is reached around 360K, whereas for Beta this value is around 390K. This has a significant impact in the adsorption process performance because the specific thermal energy ($sp_{thermal}$) and the working capacity (WC) of CO_2 as well as other adsorbent performance indicators are affected by these changes in the composition profiles.

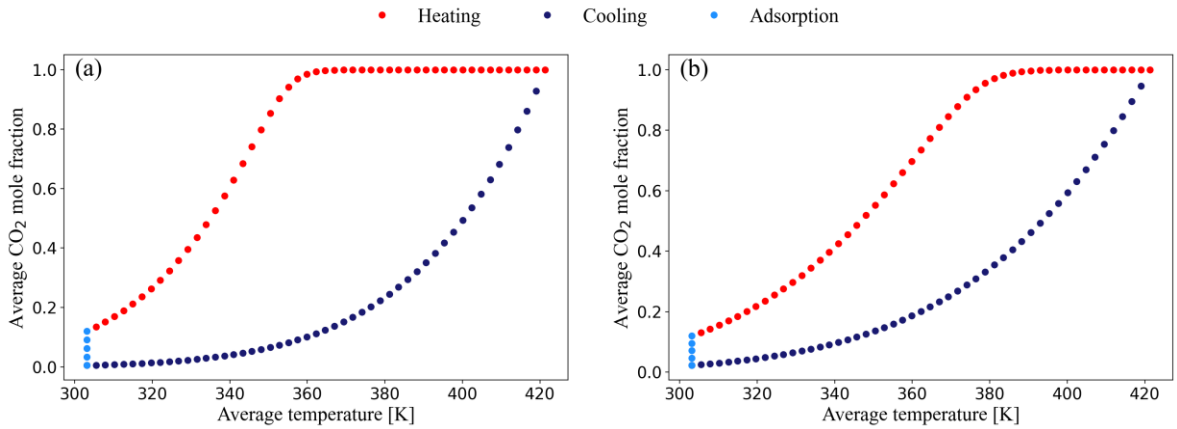

Figure 4. Cyclic steady-state bed composition profile with respect to temperature for a three-step TSA cycle. (a) NaX, (b) Beta

Equilibrium adsorption capacity can be evaluated with purity and recovery. The results for the former were 96% for NaX and 89% for Beta, and for the latter were 97% and 91% for NaX and Beta respectively, showing that NaX has a better equilibrium adsorption capacity than Beta. These results are related to the fact that NaX has a higher surface area and pore volume than Beta [28]. Nevertheless, the adsorbents' energy performance in the case study process was estimated. NaX has a specific thermal energy of 2.07 MW per kg of CO_2 and a working capacity of 2.74 molCO_2 per kg of adsorbent compared with 2.37 MW per kgCO_2 and 1.94 molCO_2 per kg of adsorbent for Beta. This means that NaX has a lower energy requirement for the stablished process conditions. Both adsorbents studied have a better energy performance than the benchmark capture technology, absorption by MEA, which presents ranges between 3.1 and 16 MW per kg of CO_2 for the heat duty [44], the correspondent to the specific thermal energy in absorption processes. Please note that the objective of this work was not to propose the optimal adsorbent for the CO_2 removal process but instead to develop a simple and reliable tool to compare among adsorbents by considering their application in industrial removal of CO_2. This model allows to evaluate different adsorbents reducing computational and mathematical complexity.

4. Benchmarking

Zeolite NaX could have even a higher recovery and purity than zeolite Beta. However, since both adsorbents can achieve the capture efficiency proposed at the stablished process conditions (90%, see Table 1), these values should not be used as criteria to select NaX over Beta for the practical application of CCUS. Not in all cases the relationship between the recovery and purity with the energetic performance is a direct one [45]. There is an

optimal range between adsorption and desorption temperatures where the adsorbent reaches its highest performance [30], but this range is different for all adsorbents. Therefore, it is imperative to stablish a capture efficiency in thermodynamic terms in order to have a reliable comparison method.

Starting from the CO_2 feed and capture efficiency proposed in Table 1, the amount of CO_2 recovered $(N_{CO_2,recovered})$ per second is 164.41 kg/s, therefore the external energy required, Q_{ext}, is given by

$$Q_{ext} = sp_{thermal} \cdot N_{CO_2,recovered} + sp_{cooling} \cdot N_{CO_2,recovered} \quad (9)$$

Note that Q_{ext} is the total amout of energy required to recover 164.41 kg/s, so the energy penalty could be defined as

$$E_{\text{penalty}} = \frac{Q_{ext}}{N_{CO_2,recovered}} \times W_{CO_2} \quad (10)$$

Where W_{CO_2} is the molar mass of CO_2.

Starting from eq 9 and eq 10, Q_{ext} is 340.33 MW and 389.65 MW for NaX and Beta respectively, and energy penalty is 91.08 MW per molCO_2 recovered for NaX and 104.28 MW per molCO_2 recovered for Beta. Therefore, NaX has a lower energy requirement than Beta for the stablished process conditions.

Note that under different conditions, Beta could have a better performance, and thus for every particular case the specific conditions should be evaluated. Bringing the process conditions to the optimal ranges of each adsorbent can lead to a higher energy demand due to the external energy required to reach these conditions. Therefore, to compare among adsorbents by considering their application in industrial removal of CO_2, it is necessary to evaluate realistic process conditions.

The energy penalty and working capacity calculated at stablished process conditions were compared for both zeolites NaX and Beta in Figure 5. These two metrics are independent of CO_2 removed, and when this is fixed, energy penalty and working capacity indicate the energy required to achieve that CO_2 removal. It is seen that in general an increase in CO_2 captured per cycle also results in a higher specific thermal energy demand. From a thermodynamic point of view, the best adsorbent should be in the upper left in Figure 5. Therefore, zeolite NaX shows an excellent compromise between the high working capacity and low specific thermal energy.

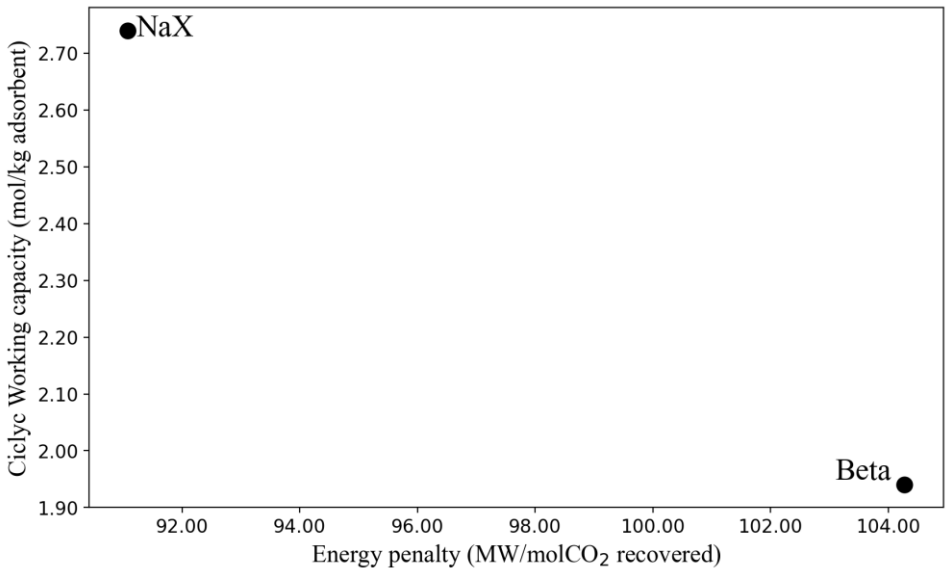

Figure 5. Performance indicators for zeolites NaX and Beta.

Finally, it is important to mention that increasing TSA cycle complexity by adding additional steps such as recycle, purge, and secondary heating steps could lead to significant improvements in performance. Specifically, for a simple TSA cycle for post-combustion carbon capture in which CO_2 purity and recovery of 83 and 80% are attained, introducing additional steps could lead to improvements of over 15% in purity and recovery [46].

5. Conclusions

Adsorption and desorption isotherm models for zeolites NaX and Beta were modeled based on individual experimental data using the Dual-Site Langmuir isotherm. The models had excellent agreement to the experimental data, with a maximum MRE sum of 0.051 and 0.063 for zeolite NaX and Beta respectively. The binary adsorption predicted by DSL showed the nonideal behavior of CO_2/N_2 mixture and good capacity of these adsorbents. Likewise, mass and heat transfer for CO_2 and N_2 in a TSA cycle were simulated using a shortcut-model at realistic process conditions, showing higher equilibrium adsorption capacity for NaX, with a purity and recovery of 96 and 97 % respectively compared with 89 and 91 % for Beta. This can be expected due to the fact that NaX has a highest surface area and pore volume.

Also, the model developed in this work allowed to compare two commonly used adsorbents to evaluate their energy performance in the CO_2 capture process. The working capacity and specific thermal energy were evaluated and proposed an accurate benchmark to compare among adsorbent in terms of their process performance instead of their properties. NaX presented lower energy requirement than Beta for the stablished process conditions, with 13% less energy penalty, and 29% more working capacity.

References

[1] International Energy Agengy (IEA), "CO2 Emissions from Fuel Combustion: Overview," 2020. [Online]. Available: https://www.iea.org/reports/co2-emissions-from-fuel-combustion-overview. [Accessed 21 August 2020].

[2] A. S. U. M. K. D. y. J. Z. K. Zeeshan, "Consumption-based carbon emissions and International trade in G7 countries: The role of Environmental innovation and Renewable energy," *Science of the Total Environment,* vol. 730, no. 138945, 2020.

[3] National Oceanic and Atmospheric Administration (NOAA), "Global Climate Change Indicators, National Centers For Environmental Information (NCEI)," 2020. [Online]. Available: https://www.ncdc.noaa.gov/monitoring-references/faq/indicators.php. [Accessed 22 August 2020].

[4] The Royal Society, "Is the climate warming?," March 2020. [Online]. Available: https://royalsociety.org/topics-policy/projects/climate-change-evidence-causes/question-1/. [Accessed 30 October 2021].

[5] J. P. Laboratory, "Ramp-Up in Antarctic Ice Loss Speeds Sea Level Rise, NASA," 13 June 2018. [Online]. Available: https://www.jpl.nasa.gov/news/news.php?feature=7159. [Accessed 22 August 20].

[6] National Snow & Ice Data Center,, "State of the cryosphere," 19 June 2019. [Online]. Available: https://nsidc.org/cryosphere/sotc/glacier_balance.html. [Accessed 22 August 2020].

[7] International Energy Agency (IEA), World energy outlook 2018, Paris: International Energy Agency, 2018.

[8] International Energy Agency (IEA), Renewable Power, Paris: International Energy Agency, 2020.

[9] T. F. S. P. H. M. y. R. D. S. J. D. Figueroa, "Advances in CO2 capture technology—The U.S. Department of Energy's Carbon Sequestration Program," *International Journal of Greenhouse Gas Control,* vol. II, no. 1, pp. 9-20, 2008.

[10] Z. L. P. L. J. Y. y. A. E. R. L. Wanga, "Experimental and modeling investigation on post- combustion carbon dioxide capture using zeolite 13X-APG by hybrid VTSA process," *Chemical Engineering Journal,* vol. 197, pp. 151-161, 2012.

[11] E. G. W. L. L. F. V. y. J. B. P. C. O. Arean, "Carbon dioxide and nitrogen adsorption on porous copolymers of divinylbenzene and acrylic acid," *Adsorption,* vol. 19, p. 367–372, 2013.

[12] International Energy Agency (IEA), The role of CCUS in low-carbon power systems, Paris: International Energy Agency, 2020.

[13] X. J. y. X. L. Y. Zhang, "Energy consumption analysis for CO2 separation from gas mixtures," *Applied Energy*, vol. 130, pp. 237-243, 2014.

[14] T. W. M. J. B. E. J. A. A.-H. A. P. R. W. H. P. A. W. y. J. Y. Z. Zhang, "Advances in carbon capture, utilization and storage," *Applied Energy*, vol. 278, 2020.

[15] J. Wilcox, "Introduction to Carbon Capture," Carbon Capture, New York, Springer, 2012.

[16] B. A. O. y. G. T. Rochelle, "Alternative stripper configurations for CO2 capture by aqueous amines," *AICHE Journal*, vol. 53, p. 3144–3154, 2007.

[17] E. T. H. y. M. T. H. F. Svendsen, "Carbon dioxide capture by absorption, challenges and possibilities," *Chemical Engineering Journal*, vol. 171, no. 3, pp. 718-724, 2011.

[18] W. M. Budzianowski, "Single solvents, solvent blends, and advanced solvent systems in CO2 capture by absorption: a review," *International Journal of Global Warming*, vol. 7, p. 184–225, 2015.

[19] S. F. I. A. K. M. S. M. C. Q. y. R. A. S. Vasudevan, "Energy penalty estimates for CO2 capture: Comparison between fuel types and capture-combustion modes," *Energy*, vol. 103, pp. 709-714, 2016.

[20] V. R. R. S. G. P. S. R. H. A. R. M. A. S. Krishnamurthy, "CO2 Capture from Dry Flue Gas by Vacuum Swing Adsorption: A Pilot Plant Study," *American Institute of Chemical Engineers*, vol. 60, no. 5, pp. 1830-1842, 2014.

[21] P. Shirley and P. Myles, "Quality Guidelines for Energy System Studies: CO2 Impurity Design Parameters," USDOE Office of Fossil Energy, Pittsburgh, 2019.

[22] N. Berenstein, "Making a global sensation: Vanilla flavor, synthetic chemistry, and the meanings of purity," *SAGE Journals*, vol. 54, no. 4, pp. 399-424, 2016.

[23] L. W. X. K. P. L. y. J. R. A. E. Y. Z. Liu, "Onsite CO2 Capture from Flue Gas by an Adsorption Process in a Coal-Fired Power Plant," *Industrial & Engineering Chemistry Research*, vol. 51, no. 21, p. 7355–7363, 2012.

[24] P. X. D. X. y. P. A. W. G. Li, "Dual mode roll-up effect in multicomponent non-isothermal adsorption processes with multilayered bed packing," *Chemical Engineering Science*, vol. 66, no. 9, pp. 1825-1834, 2011.

[25] A. M. V. y. G. N. Karanikolos, "CO2 capture adsorbents functionalized by amine – bearing polymers: A review," *International Journal of Greenhouse Gas Control*, vol. 96, no. 103005, 2020.

[26] J. A. S. y. A. R. N. S. Wilkins, "Measurement of competitive CO2 and H2O adsorption on zeolite 13X for post-combustion CO2 capture," *Adsorption*, vol. 25, p. 115–133, 2019.

[27] W. Z. X. C. Q. X. y. Z. L. Z. Zhang, "Adsorption of CO2 on Zeolite 13X and Activated Carbon with Higher Surface Area," *Separation Science and Technology*, vol. 45, pp. 710-719, 2010.

[28] M. M. y. C.-H. L. E. Khoramzadeh, "Equilibrium Adsorption Study of CO2 and N2 on Synthesized Zeolites 13X, 4A, 5A, and Beta," *Journar of chemical & engineering data*, vol. 64, no. 12, pp. 5648-5664, 2019.

[29] J.-H. K. J.-T. K. J.-K. S. J.-M. L. y. C.-H. L. J.-S. Lee, "Adsorption Equilibria of CO2 on Zeolite 13X and Zeolite X/Activated Carbon Composite," *Journal of chemical & engineering data*, vol. 47, pp. 1237-1242, 2002.

[30] A. Ajenifuja, L. Joss and M. Jobson, "A New Equilibrium Shortcut Temperature Swing Adsorption Model for Fast Adsorbent Screening," *Industrial & Engineering Chemistry Research*, vol. 59, no. 8, pp. 3485-3497, 202.

[31] Y. S. y. N. C. X. Zhu, "Integrated gasification combined cycle with carbon dioxide capture by elevated temperature pressure swing adsorption," *Applied Energy*, vol. 176, pp. 196-208, 2016.

[32] M. H. O. B. M. B. N. Q. A. P. T. L. y. M. A. R. Ben-Mansour, "Carbon capture by physical adsorption: Materials, experimental investigations and numerical modeling and simulations – A review," *Applied Energy*, vol. 161, no. 1, pp. 225-255, 2016.

[33] P. A. y. R. C. F. Raganati, "CO2 adsorption on fine activated carbon in a sound assisted fluidized bed: Effect of sound intensity and frequency, CO2 partial pressure and fluidization velocity," *Applied Energy*, vol. 113, pp. 1269-1282, 2014.

[34] L. Y. J. W. Z. Z. W. Q. D. L. y. L. L. M. Wang, "Adsorption and regeneration study of polyethylenimine-impregnated millimeter-sized mesoporous carbon spheres for post-combustion CO2 capture," *Applied Energy*, vol. 168, no. 15, pp. 282-290, 2016.

[35] J. L. X. W. J. D. H. F. J. Y. y. J. Y. W. Wang, "Carbon dioxide adsorption thermodynamics and mechanisms on MCM-41 supported polyethylenimine prepared by wet impregnation method," *Applied Energy*, vol. 142, no. 15, pp. 221-228, 2015.

[36] T. Sanpasertparnich, R. Idem, I. Bolea, D. deMontigny and P. Tontiwachwuthikul, "Integration of post-combustion capture and storage into a pulverized coal-fired power plant," *International Journal of Greenhouse Gas Control,* vol. 4, p. 499–510, 2010.

[37] W. L. McCabe, J. C. Smith and P. Harriott, Unit operations of chemical engineering, New York: McGraw-hill, 1993.

[38] I. Langmuir, "THE ADSORPTION OF GASES ON PLANE SURFACES OF GLASS, MICA AND PLATINUM.," *Journal of the American Chemical Society,* vol. 40, no. 9, pp. 1361-1403, 1918.

[39] J. A. Ritter, S. J. Bhadra and A. D. Ebner, "On the Use of the Dual-Process Langmuir Model for Correlating Unary Equilibria and Predicting Mixed-Gas Adsorption Equilibria," *Langmuir,* vol. 27, no. 8, pp. 4700-4712, 2011.

[40] S. J. Bhadra, A. D. Ebner and J. A. Ritter, "On the Use of the Dual Process Langmuir Model for Predicting Unary and Binary Isosteric Heats of Adsorption," *Langmuir,* vol. 28, no. 17, pp. 6935-6941, 2012.

[41] S. García, J. J. Pis, F. Rubiera and C. Pevida, "Predicting Mixed-Gas Adsorption Equilibria on Activated Carbon for Precombustion CO2 Capture," *Langmuir,* vol. 29, no. 20, pp. 6042-6052, 2013.

[42] M. Jaschik, M. Tanczyk, J. Jaschik and A. Janusz-Cygan, "Data concerning adsorption equilibria of carbon dioxide, nitrogen and oxygen over a zeolite molecular sieve 13X for the modelling of carbon dioxide capture from gaseous mixtures by adsorptive processes," *Data in brief,* vol. 30, p. 105638, 2020.

[43] D. M. Ruthven, S. Farooq and K. S. Knaebel, Pressure swing adsorption, New York: VCH Publishers, 1994.

[44] L. M. Romeo, D. Minguell, R. Shirmohammadi and J. M. Andrés, "Comparative Analysis of the Efficiency Penalty in Power Plants of Different Amine-Based Solvents for CO2 Capture," *Industrial & Engineering Chemistry Research* , vol. 59, no. 21, pp. 10082-10092, 2020.

[45] B. J. Maring and P. A. Wembley, "A new simplified pressure/vacuum swing adsorption model for rapid adsorbent screening for CO2 capture applications," *International Journal of Greenhouse Gas Control,* vol. 15, pp. 16-31, 2013.

[46] L. Joss, M. Gazzanu and M. Mazzotti, "Rational design of temperature swing adsorption cycles for post-combustion CO2 capture," *Chemical Engineering Science,* vol. 158, no. 2, pp. 381-394, 2017.

[47] E. Khoramzadeh, M. Mofarahi and C.-H. Lee, "Equilibrium Adsorption Study of CO2 and N2 on Synthesized Zeolites 13X, 4A, 5A, and Beta," *Journal of Chemical & Engineering Data,* vol. 64, no. 12, pp. 5648-5664, 2019.

[48] H. D. X. T. Q. Y. X. Z. y. H. L. H. Yi, "«Adsorption equilibrium and kinetics for SO2, NO, CO2 on zeolites FAU and LTA,»," *Journal of Hazardous Materials,* vol. 1, no. 2203-204, pp. 111- 117, 2012.